Three-Dimensional Resonant Coherent Excitation of Nonchanneling Ions in a Crystal

C. Kondo,[1,2,3,*] S. Masugi,[3] Y. Nakano,[3] A. Hatakeyama,[1] T. Azuma,[3] K. Komaki,[1]
Y. Yamazaki,[1,2] T. Murakami,[4] and E. Takada[4]

[1]*Graduate School of Arts and Sciences, University of Tokyo, Komaba, Meguro, Tokyo 153-8902, Japan*
[2]*Atomic Physics Laboratory, RIKEN, Wako, Saitama 351-0198, Japan*
[3]*Department of Physics, Tokyo Metropolitan University, Hachioji, Tokyo 192-0397, Japan*
[4]*National Institute of Radiological Science, Inage, Chiba 263-8555, Japan*

(Received 12 July 2006; published 26 September 2006)

We have observed resonant coherent excitation (RCE) of H-like Ar^{17+} ions traveling through a 1 μm-thick Si crystal at an energy of 391 MeV/u in the nonchanneling condition. A three-dimensional periodic array of atomic planes induces RCE of the nonchanneling ions. The high energy heavy ions together with the thin crystal allow us to observe this new RCE through the measurements of the charge-state distribution of the emerging ions. The observed resonances are much narrower than those of planar-channeling ions due to the absence of the large Stark shift caused by the planar potential.

DOI: 10.1103/PhysRevLett.97.135503 PACS numbers: 61.85.+p, 32.60.+i, 34.50.Fa

An energetic ion injected into a single crystal in the direction parallel to atomic strings or atomic planes of the crystal moves in open spaces between the strings or the planes without suffering severe collisions with target nuclei and electrons. This phenomenon is called ''channeling''. In addition, the ion passing through the single crystal feels temporally oscillating fields originating from the spatially periodic structure. When one of the frequencies corresponds to the transition energy of the ion, the oscillating field has a chance to resonantly excite the internal state of the ion. This process, called ''resonant coherent excitation'' (RCE), was first pointed out by Okorokov [1] in 1965, and was observed by Datz *et al*. [2] for the first time through the exit charge-state distribution of axial-channeling ions in 1978. Since then many experiments have been performed using low $Z(\leq 14)$ and low energy ($\sim$ MeV/u) ions in the axial- or planar-channeling condition, or in the surface-scattering condition [3,4]. As shown in Fig. 1(a) and 1(b), RCEs in the axial- and planar-channeling conditions are induced by a periodic array of atoms along a (one-dimensional) atomic string and by that of atomic strings on a (two-dimensional) atomic plane, respectively. In this context, we may refer to RCE in the axial-channeling condition as ''1D RCE'' and that in the planar-channeling condition as ''2D RCE''. Their features are asymmetric and structured resonance profiles due to the Stark shifts induced by the dynamical wake potential and the static axial or planar potential in the channels. These Stark shifts depend on the ion trajectory determined by the static potential in the crystal, and result in the complicated resonance profiles.

The channeling condition has been required in these experiments to suppress collisions with the crystal atoms, which destroy coherence between the ion states relevant to the transition. This is particularly essential for low Z and low energy ions. However, the ions traveling in arbitrary directions also feel the crystal field oscillating. In principle, RCE does not require the channeling conditions [5]. We report in this Letter the first observation of RCE in the nonchanneling condition by employing a combination of heavy ions (H-like Ar^{17+}) with high, moderately relativistic, energy (391 MeV/u) and a thin crystal (1 μm-thick Si). The high energy suppresses decoherence processes caused by the collisions even in the nonchanneling condition, and the thin crystal enables us to observe the resonances through the measurements of the exit charge-state distribution of the ions. This RCE is induced by a three-dimensional (3D) periodic array of atomic planes in a crystal as shown in Fig. 1(c). We hereafter refer to this new RCE as ''3D RCE''. 3D RCE inherently has no trajectory dependence of atomic processes, such as the RCE and ionization probabilities and the Stark shift, as a natural consequence of the nonchanneling condition, in contrast to 1D and 2D RCEs. In addition, the planar potential that has induced the large static Stark shift for the channeling ions is not static any more but oscillating for the nonchanneling ions. The frequency of this additional oscillating field is too high for the ion states to adjust, and the resulting ac Stark shift is small. We note that the Stark shift induced by the wake potential is small enough to ignore in this high energy region. Indeed, the observed resonance profiles of 3D RCE turned out to be sharp and symmetric compared with those of 2D RCE in the same crystal. 3D RCE is ideal to study the nature of RCE free from the complicated situation inevitable in 1D and 2D RCEs.

The resonance condition for the transition energy ΔE is given by $\Delta E = h\nu$, where h is Planck's constant and ν is the frequency of the oscillating field induced by an array of atomic planes in the case of 3D RCE. When the array is specified by the reciprocal lattice vector $\mathbf{g}$, the frequency ν is expressed as $\gamma\mathbf{g}\cdot\mathbf{v}$, where γ is the Lorentz factor and $\mathbf{v}$ the ion velocity vector. In the present experiment with a Si crystal (diamond structure), we define a new set of base lattice vectors to be $\mathbf{A} = (-1, 1, 0)a/2$, $\mathbf{B} = (0, 0, 1)a$, and $\mathbf{C} = (1, 1, 0)a/2$ (a: lattice constant) in the original cubic coordinate system, and the base vectors of the reciprocal

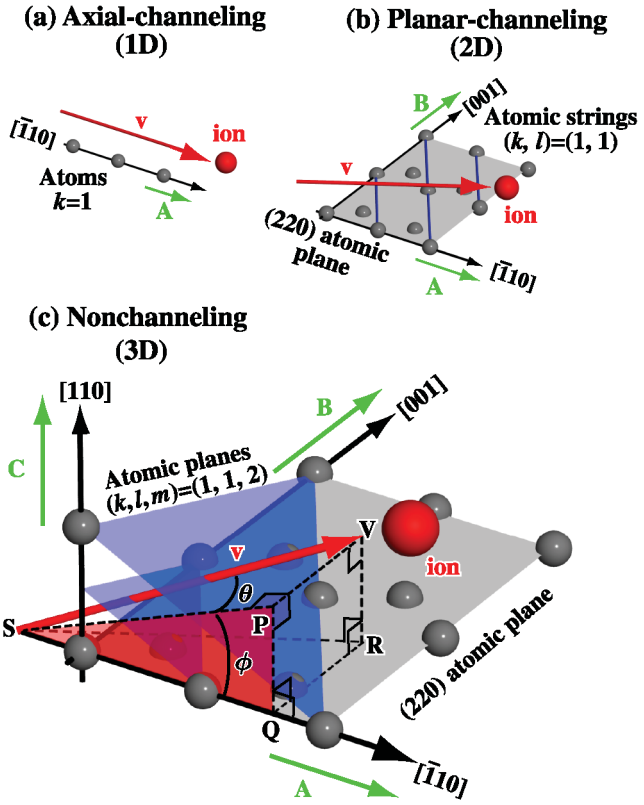

FIG. 1 (color). Configurations of the ion velocity $\mathbf{v}$ in a Si crystal. Three kinds of periodic arrays are shown: (a) atoms in an atomic string (1D) in the $[\bar{1}10]$ axial-channeling condition; (b) atomic strings on an atomic plane (2D) in the (220) planar-channeling condition; (c) atomic planes in the crystal (3D) in the nonchanneling condition. **A**, **B**, and **C** represent the base lattice vectors. The (220) atomic plane is spanned by **A** and **B**, and the (004) atomic plane by **A** and **C**. $\overrightarrow{SP}$ and $\overrightarrow{SR}$ are the projections of $\mathbf{v}(\overrightarrow{SV})$ on the (004) and (220) atomic planes. $\overrightarrow{SQ}$ is the projection of $\overrightarrow{SP}$ on the $[\bar{1}10]$ axis. θ is the angle between $\overrightarrow{SV}$ and $\overrightarrow{SP}$, ϕ between $\overrightarrow{SP}$ and $\overrightarrow{SQ}$.

lattice are expressed as $\mathbf{A}^* = (-1, 1, 0)/a$, $\mathbf{B}^* = (0, 0, 1)/a$, and $\mathbf{C}^* = (1, 1, 0)/a$. A reciprocal lattice vector is then represented by $\mathbf{g} = k\mathbf{A}^* + l\mathbf{B}^* + m\mathbf{C}^*$, where (k, l, m) is the Miller index specifying an array of atomic planes in terms of the new set of base vectors. As shown in Fig. 1(c), we define the angle of the ion velocity with respect to the (004) atomic plane as θ, and the angle of the ion velocity projected on the (004) atomic plane with respect to the $[\bar{1}10]$ axis as ϕ. The ion velocity is expressed as $\mathbf{v} = v(\hat{\mathbf{A}}\cos\theta\cos\phi + \hat{\mathbf{B}}\sin\theta + \hat{\mathbf{C}}\cos\theta\sin\phi)$, where v is the absolute value of the velocity, and $\hat{\mathbf{A}}$, $\hat{\mathbf{B}}$, $\hat{\mathbf{C}}$ are the unit vectors along **A**, **B**, **C**, respectively. Accordingly, the resonance condition is obtained as,

$$\Delta E = h\nu = \frac{h\gamma v}{a}\{\sqrt{2}(k\cos\phi + m\sin\phi)\cos\theta + l\sin\theta\}. \quad (1)$$

We can readily prepare the resonance condition by varying the angles θ and ϕ, keeping the ion velocity v constant. When $\phi = 0°$, the incident direction of the ion satisfies the (220) planar-channeling condition regardless of θ. It is also noted that the extinction rule of the resonance, which originates from the destructive interference of the oscillating fields, is $k + l + m =$ odd or $2k + l = 4j + 2$, where j is an integer [6,7].

We investigated the 3D RCE of a $1s$ electron to the $n = 2$ states in H-like Ar^{17+} ions through the measurements of the exit charge-state distribution of the ions as functions of the angles θ and ϕ by tilting the crystal. The beam energy was evaluated to be 391.07 MeV/u, which will be discussed later. Figure 2 bottom shows the relation between θ and ϕ satisfying the resonance conditions for the $1s$-$2p$ transitions with the transition energies in vacuum in the investigated range of the angles θ and ϕ. In the planar-channeling condition, the two points on the line of $\phi = 0°$ satisfy the 2D RCE conditions for the $1s$-$2p_{1/2}$ and $1s$-$2p_{3/2}$ transitions. They are specified by the 2D Miller index $(k, l) = (1, 1)$. As deviating from the planar-channeling condition by increasing ϕ, each resonance condition splits into several lines corresponding to the additional Miller index m.

The experimental setup was described in detail elsewhere [7,8]. The experiments were performed at the Heavy Ion Medical Accelerator in Chiba (HIMAC). A 50 mm-thick collimator with a hole of 0.6 mm in diameter, and a 50 mm-thick horizontal slit of 0.2 mm in width were located 650 cm and 50 cm upstream of the target crystal, respectively. The ions were injected into the Si crystal mounted on a three-axis goniometer. The charge-state distribution of the emerging ions was measured with a combination of a charge separation magnet and a 2D position-sensitive Si detector located 120 cm and 550 cm downstream of the target, respectively. The beam divergence was 0.04 mrad, evaluated by the beam profile on the 2D detector and the configuration of the beam transport.

The thickness of the Si target was measured to be 1.0 μm by the energy loss of alpha particles emitted from ^{241}Am. This thickness is crucial for the observation of 3D RCE as a decrease of the survived Ar^{17+} fraction. The mean free paths of collisional ionization of the Ar^{17+} ions are estimated to be 4.3 μm for the nonexcited ($1s$) ions and 1.0 μm for the excited ($2p$) ions, respectively [9]. This means that a large fraction of the nonexcited ions survive from ionization, while a significant fraction of the excited ions are ionized during the travel in the 1.0 μm-thick Si.

We first investigated ϕ dependence of the survived Ar^{17+} fraction of the emerged ions under the non-RCE condition. In the (220) planar-channeling condition ($\phi = 0.000°$), the fraction was 0.83. It decreased to 0.67 at $\phi = 0.015°$. At $\phi > 0.020°$, where the ions were not channeling, the fraction took a constant value of 0.72, which was well reproduced by the theoretical estimation [9].

We next measured the 2D RCE profile, i.e., the survived Ar^{17+} fraction as a function of θ in the (220) planar-channeling condition (keeping $\phi = 0.000°$). The fraction

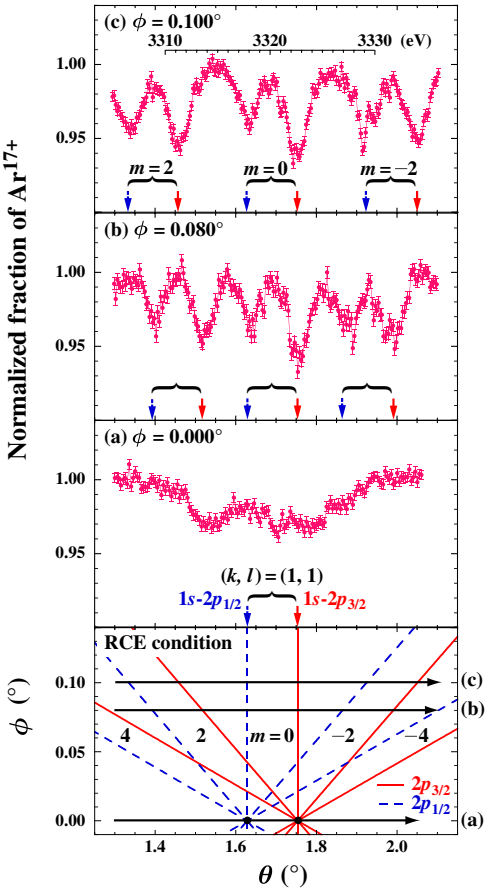

FIG. 2 (color online). Bottom—the resonance conditions of $1s\text{-}2p_{1/2}$ (dashed line) and $1s\text{-}2p_{3/2}$ (solid line) transitions of the 391.07 MeV/u H-like Ar^{17+} ion for $(k, l, m) = (1, 1, m)$ ($m = -4, -2, 0, 2, 4$). The horizontal arrows indicate the scanned regions in the present experiment. The survived fraction of H-like Ar^{17+} ions measured as a function of θ keeping (a) $\phi = 0.000°$, the (220) planar-channeling condition, and (b) $\phi = 0.080°$, (c) $\phi = 0.100°$, the nonchanneling conditions. The survived fraction is normalized to the value in the non-RCE condition. The vertical arrows on the lower axes indicate the resonance conditions for $1s\text{-}2p_{1/2}$ and $1s\text{-}2p_{3/2}$. The additional scale in (c) is the transition energy calculated with Eq. (1) for $(k, l, m) = (1, 1, 0)$.

normalized to the non-RCE value is shown in Fig. 2(a). The normalized fraction decreases by 3% at maximum on resonance. The resonance exhibits a broad and shallow profile. The fine structure of the $2p_{1/2}$ and $2p_{3/2}$ states, previously observed in the same conditions except the crystal thickness (21 and 94.7 μm), is not resolved clearly [10,11]. We here give a qualitative explanation of this difference as follows. The ions traveling close to the (220) atomic planes have large probabilities of RCE and the subsequent ionization compared to the ions in the channel center. Furthermore, these ions suffer the large Stark shift (~5 eV at maximum [7]) due to the coupling between the $2s$ and $2p$ states, which leads to the broadening of the resonance profile for the thin crystal. As the crystal thickness increases, the resonance profile gets deeper. However, the contribution to the profile from the ions close to the atomic planes saturates, and the role of the ions in the channel center is, in turn, emphasized. As a result, the fine structure is resolved.

We proceeded to the measurement of the 3D RCE resonance profiles as a function of θ in the nonchanneling conditions (keeping $\phi = 0.080°$ and $0.100°$). As shown in Figs. 2(b) and 2(c), we found three pairs of distinct decreases of the normalized fraction due to 3D RCE corresponding to $(k, l, m) = (1, 1, 2)$, $(1, 1, 0)$, and $(1, 1, -2)$. The maximum decrease amounts to 7% at $\phi = 0.100°$. The deeper resonance of $2p_{3/2}$ than $2p_{1/2}$ is basically explained by the higher multiplicity of the $2p_{3/2}$ state.

The remarkable feature of 3D RCE is the drastic narrowing of the resonance profile compared with 2D RCE. Namely, the static Stark shifts of the $2p_{1/2}$ and $2p_{3/2}$ states due to the coupling to the $2s$ state disappear in the nonchanneling condition. It is explained by the fact that the electric field derived from the (220) planar potential, which induces the static Stark shift for the channeling ions, acts as a rapidly oscillating field on the nonchanneling ions, since the ions traverse the (220) atomic planes many times as shown in Fig. 3. This oscillating field induces the ac Stark shift, which is, however, small because the frequency of the field is far from the energy differences between the $2s$ and $2p$ states. We roughly estimate this small shift in the framework of the standard perturbative treatment of the ac stark shift [12]. The ions in the nonchanneling condition feel the (220) planar field as

$$F(t) = \sum_{m=2}^{+\infty} F_m \sin(2\pi\nu_m t) \qquad (m\text{: even}). \tag{2}$$

F_m is the Fourier component corresponding to the $(k, l, m) = (0, 0, m)$ planes. The frequency ν_m is derived from Eq. (1) as $(\gamma v/a)\sqrt{2}m\cos\theta\sin\phi$. The ac stark shift caused by this field is expressed as

$$\delta E = \sum_{m=2}^{+\infty} \frac{|d_z F_m|^2}{2} \frac{\Delta}{\Delta^2 - (h\nu_m)^2} \qquad (m\text{: even}), \tag{3}$$

where d_z is the component of the dipole matrix element between the $2s$ and $2p$ states along the direction of the (220) planar field (z direction). Note that d_z for the $2p_{3/2}$ ($|j_z| = 3/2$) states is zero. Δ is the energy difference of $2p$ from $2s$. F_m is derived from the crystal potential. We assume that it is represented by a sum of atomic potentials, for which we adopted the Moliére potential with thermal vibration folded. Hereafter, we consider the case of $\phi = 0.100°$. For $m = 2$, the frequency ν_2 corresponds to 11.4 eV, and $d_z F_2$ for the $2p_{1/2}$ and $2p_{3/2}$ ($|j_z| = 1/2$) states are estimated to be 2.3 eV and 3.1 eV in the projectile frame. Then, using $\Delta = -0.16$ and 4.7 eV for the $2p_{1/2}$ and $2p_{3/2}$ ($|j_z| = 1/2$) states [13], the shifts are evaluated to be 0.0033 and -0.21 eV, respectively. The higher m components make only a minor contribution. Thus, we do understand that the shift in the nonchanneling condition is

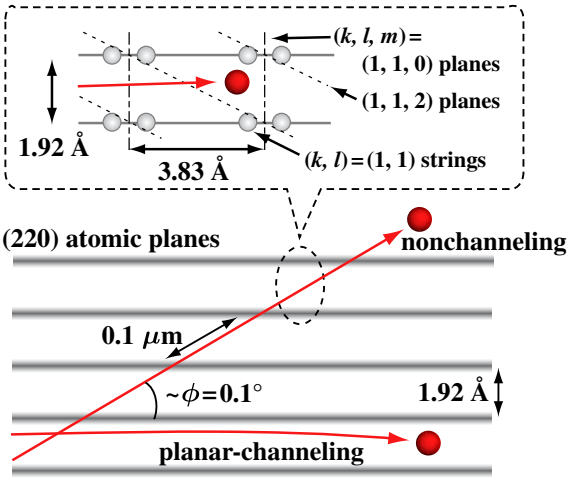

FIG. 3 (color online). Schematic cross section of the crystal at the plane SVR defined in Fig. 1. The trajectories of the nonchanneling ion at $\phi = 0.100°$ and the (220) planar-channeling ion are shown. The enlarged sketch shows the atomic strings of $(k, l) = (1, 1)$ and the atomic planes of $(k, l, m) = (1, 1, 0)$ and (1,1,2). When θ is small, ϕ is nearly equal to the incident angle of the ions with respect to the (220) atomic plane.

much smaller than that in the channeling condition. It is to be pointed out that the present perturbative treatment cannot be applied at smaller angles of ϕ where the frequencies ν_m approach the energy difference between $2s$ and $2p_{1/2,3/2}$. Generally, the traveling ions feel many oscillating fields with a variety of frequencies in the crystal simultaneously. It is possible to make two such frequencies satisfy the 3D RCE conditions for different transitions by varying the angles θ and ϕ, keeping the ion velocity constant. That is, a double resonance can be realized, and we indeed observed quite characteristic profiles, which will be reported separately.

The full widths at half minimum of the resonance dips for $1s$-$2p_{1/2}$ and $1s$-$2p_{3/2}$ transitions at $\phi = 0.100°$ are about 2 eV. The widths originate not only from relaxation of the coherence between the $1s$ and $2p$ states, but also from the non-negligible velocity distribution and beam divergence. Thus, the widths are regarded as the upper limit of the relaxation rate of the coherence, and it is estimated to be 1.6×10^{15} s^{-1}. This rate is lower than the frequency at which the ion traverses the (220) atomic planes, indicating that the coherence of the ion is kept even when the ion goes through the high atomic density region of the (220) atomic plane.

Finally, we describe how we evaluated the beam energy. The resonance angles θ, ϕ and the transition energies ΔE give a beam energy from Eq. (1) for each resonance. We calculated beam energies for the six resonances at $\phi = 0.100°$, using the transition energies in vacuum. By averaging them, we obtained a value of 391.07 MeV/u. Note that the ac Stark shifts discussed above affect only the last digit of this beam energy.

In summary, we have succeeded in observing 3D RCE of nonchanneling ions by adopting high energy heavy ions and the thin crystal. The high energy suppresses decoherence between the ion states relevant to the transition, and the thin crystal allows us to observe the resonance in the nonchanneling condition through the measurements of the charge-state distribution of the emerging ions. The 3D resonance profile is drastically narrower than the 2D resonance profile in the planar-channeling condition. The planar potential inducing the large static Stark effect in 2D RCE is not static but oscillates in the projectile frame of the nonchanneling ion. The observed narrowing is explained by the small ac Stark shift due to this oscillating field.

We thank Dr. Y. Nakai of RIKEN for helpful discussions. This work was supported in part by Grants-in-Aid for Scientific Research (No. 13440126 and No. 16204030) from the Japan Society for the Promotion of Science and also by Matsuo Foundation. This experiment is one of the research projects with heavy ions at NIRS-HIMAC.

*Electronic address: ckondo@radphys4.c.u-tokyo.ac.jp

[1] V. V. Okorokov, JETP Lett. **2**, 111 (1965).
[2] S. Datz, C. D. Moak, O. H. Crawford, H. F. Krause, P. F. Dittner, J. Gomez del Campo, J. A. Biggerstaff, P. D. Miller, P. Hvelplund, and H. Knudsen, Phys. Rev. Lett. **40**, 843 (1978).
[3] H. F. Krause and S. Datz, Adv. At. Mol. Opt. Phys. **37**, 139 (1996).
[4] F. J. García de Abajo and V. H. Ponce, Adv. Quantum Chem. **46**, 65 (2004).
[5] O. H. Crawford and R. H. Ritchie, Phys. Rev. A **20**, 1848 (1979).
[6] H. F. Krause, S. Datz, P. F. Dittner, N. L. Jones, and C. R. Vane, Phys. Rev. Lett. **71**, 348 (1993).
[7] K. Komaki, T. Azuma, T. Ito, Y. Takabayashi, Y. Yamazaki, M. Sano, M. Torikoshi, A. Kitagawa, E. Takada, and T. Murakami, Nucl. Instrum. Methods Phys. Res., Sect. B **146**, 19 (1998).
[8] T. Azuma, T. Ito, Y. Yamazaki, K. Komaki, M. Sano, M. Torikoshi, A. Kitagawa, E. Takada, and T. Murakami, Nucl. Instrum. Methods Phys. Res., Sect. B **135**, 61 (1998).
[9] J. P. Rozet, C. Stephan, and D. Vernhet, Nucl. Instrum. Methods Phys. Res., Sect. B **107**, 67 (1996).
[10] T. Azuma, T. Ito, K. Komaki, Y. Yamazaki, M. Sano, M. Torikoshi, A. Kitagawa, E. Takada, and T. Murakami, Phys. Rev. Lett. **83**, 528 (1999).
[11] T. Azuma, Y. Takabayashi, T. Ito, K. Komaki, Y. Yamazaki, E. Takada, and T. Murakami, Nucl. Instrum. Methods Phys. Res., Sect. B **212**, 397 (2003).
[12] B. H. Bransden and C. J. Joachain, *Physics of Atoms and Molecules* (Pearson Edu., Harlow, England, 2003), 2nd ed.
[13] National Institute of Standards and Technology (NIST), *NIST Atomic Spectra Database*, http://physics.nist.gov/PhysRefData/ASD/index.html.